The structure of hypersonic shock waves using Navier-Stokes equations modified to include mass diffusion

C. J. Greenshields and J. M. Reese
Department of Mechanical Engineering, University of Strathclyde
Glasgow G1 1XJ, United Kingdom

Abstract

Howard Brenner[?,?,?] has recently proposed modifications to the Navier-Stokes equations that relate to a diffusion of fluid volume that would be significant for flows with high density gradients. In a previous paper,[?] we found these modifications gave good predictions of the viscous structure of shock waves in argon in the range Mach 1.0–12.0 (while conventional Navier-Stokes equations are known to fail above about Mach 2). However, some areas of concern with this model were a somewhat arbitrary choice of modelling coefficient, and potentially unphysical and unstable solutions. In this paper, we therefore present slightly different modifications to include molecule mass diffusion fully in the Navier-Stokes equations. These modifications are shown to be stable and produce physical solutions to the shock problem of a quality broadly similar to those from the family of extended hydrodynamic models that includes the Burnett equations. The modifications primarily add a diffusion term to the mass conservation equation, so are at least as simple to solve as the Navier-Stokes equations; there are none of the numerical implementation problems of conventional extended hydrodynamics models, particularly in respect of boundary conditions. We recommend further investigation and testing on a number of different benchmark non-equilibrium flow cases.

1. Background

A parameter which indicates the extent to which a local region of flowing gas is in thermodynamic equilibrium is the Knudsen number:

$$Kn = \frac{\lambda}{L} \approx \frac{\lambda}{\rho} |\boldsymbol{\nabla}\rho|, \tag{1}$$

where λ is the mean free path of the gas molecules, L is a characteristic length of the flow system and ρ is a characteristic mass density. As Kn increases, e.g. for vehicles travelling at hypersonic speeds or at high altitudes, the departure of the gas from local thermodynamic equilibrium increases, and the notion of the gas as a continuum-equilibrium fluid becomes less valid. The Navier-Stokes equations (with standard no-slip boundary conditions) are, for example, typically confined to cases where $Kn \lesssim 0.01$. Their underlying constitutive laws for viscous stress tensor $\boldsymbol{T}$ and heat flux $\boldsymbol{j}_e$, i.e. Newton's law and Fourier's law respectively, may be derived from the Boltzmann equation using the classical Chapman-Enskog expansion in Kn to first order. *Extended*, or *modified*, *hydrodynamics* models, such as the Burnett equations, are based on Chapman-Enskog expansions to higher orders in an attempt to extend the range of applicability of the continuum-equilibrium fluid model into the so-called 'intermediate-Kn' (or 'transition-continuum') regime where $0.01 \lesssim Kn \lesssim 1$. Extended expressions for $\boldsymbol{T}$ and $\boldsymbol{j}_e$ include the same terms to first order in Kn contained in Newton's and Fourier's laws respectively, but with the addition of numerous, more complex terms that make them notoriously unstable and costly to solve.

In 2004,[?] Howard Brenner proposed that the velocity $\boldsymbol{u}$ appearing in Newton's viscosity law is generally different from the mass velocity $\boldsymbol{u}_m$ appearing in the mass conservation equation:

$$\frac{\partial \rho}{\partial t} + \boldsymbol{\nabla} \cdot (\rho \boldsymbol{u}_m) = 0. \tag{2}$$

He subsequently related the two velocities by a *diffusive volume flux density* $\boldsymbol{j}_v = \boldsymbol{u} - \boldsymbol{u}_m$ and proposed a constitutive model relating $\boldsymbol{j}_v$ to $\boldsymbol{\nabla}\rho$, similar to Fick's law of mass diffusion.[?] From this he derived modifications to the Navier-Stokes equations in which the governing transport equations of mass, momentum and energy remained unchanged but the constitutive equations for $\boldsymbol{T}$ and $\boldsymbol{j}_e$ are augmented by additional terms.[?] The resulting equations have the form of an

extended hydrodynamics model, albeit one much less complex than the family of hydrodynamics models that includes Burnett, Grad, etc.

The viscous structure of shock waves in gases provides an obvious test case for Brenner's modifications since they become increasingly significant as $\boldsymbol{\nabla}\rho$ increases. While it is accepted that the Navier-Stokes equations fail in nearly every respect in predicting correct shock structures above about Mach 2, they do reproduce the trends in experimental and molecular dynamics simulation data significantly better when Brenner's modifications are included, delivering an excellent match in the case of the inverse density thickness.[?] It is of some concern, however, that shock solutions are nonphysical when the proportionality coefficient D_v, used in the constitutive model for volume diffusion, exceeds approximately the kinematic viscosity $v = \mu/\rho$, where μ is the dynamic viscosity. Furthermore solutions were shown to be unstable when $D_v \gtrsim 1.45v$. The imposed limit on D_v effectively dictates the choice of $D_v = v$ for which there is apparently no strong physical justification.

Nevertheless, the results do partially support Brenner's original hypothesis — which is undoubtedly viewed with scepticism by some because it challenges the fundamental equations of fluid mechanics. Particular areas of criticism are that the underlying theory lacks a sound physical basis and is based on the notion of a diffusive volume flux which is somewhat difficult to conceptualise and for which constitutive models and their coefficients are untested. However, support can be found in the phenomenological GENERIC theory presented by Hans Christian Öttinger.[?] Öttinger questions why a diffusive transport term exists for both energy and momentum but not mass in the conventional Navier-Stokes equations and argues "something is missing", namely the ability of mass diffusion to produce entropy. When dissipative terms associated with mass density are identically zero, the GENERIC formulation arrives at the standard Navier-Stokes equations but, by including non-zero terms, a revised set of governing equations is derived that includes two velocities, similar to $\boldsymbol{u}_m$ and $\boldsymbol{u}$. The modifications are simply due to mass diffusion rather than the difficult concept of a diffusive volume flux.

Brenner subsequently adopted[?] the equations of Öttinger which differ from his original modifications particularly in that $\boldsymbol{u}$ appears not only in Newton's viscosity law but in the definition of momentum density itself. The purpose of this present paper is to provide additional argument in favour of the inclusion of mass diffusion and to examine its impact on the governing equations in detail. We assess the stability of the underlying equations and their ability to predict the structure of shock waves.

2. Mass diffusion and conservation

Thermal agitation causes molecules to travel from one region of a gas to another. Inequalities in molecular distribution and thermal velocity tend to be smoothed by an inevitable net migration of molecules towards regions of lower molecular concentration and/or temperature. This is the process by which mass diffuses and, in the simplest case of a single specie gas, a diffusive flux $\boldsymbol{j}_d$ occurs in the direction of negative density gradient, expressed through Fick's law simply as $\boldsymbol{j}_d = -D_m\boldsymbol{\nabla}\rho$ where D_m is the coefficient of mass diffusion (self-diffusion, in the case of a single specie gas). The conventional governing equations clearly omit the process of mass diffusion due to *net* migration of molecules by thermal agitation because they do not contain Fick's or any other constitutive model in the equation of conservation of mass. This is important in extended hydrodynamic modelling of hypersonic flows because the omission becomes more significant as $\boldsymbol{\nabla}\rho$ and, thus, Kn become larger.

Modelling of mass diffusion is, of course, a common feature in the analysis of multicomponent fluid systems. The usual approach is to retain the conservation equation for total fluid mass given by (2) and create additional conservation equations for the mass of individual gas species that each include a diffusive mass flux term.[?] However, for N gas species, only $N - 1$ equations of specie mass conservation are independent because the sum of all N equations gives (2). This means that mass diffusion is not modelled for one of the species, a statement that applies to the case of a single specie gas described in the previous paragraph. It happens because (2) *defines* $\rho\boldsymbol{u}_m$ to be the *total* mass flux density, i.e. the sum of the bulk, advective mass flux of the fluid and the net sum of diffusive mass flux of all consitutents of the fluid. In other words, $\boldsymbol{u}_m$ constitutes a mean, or local mass average, velocity of all consitutents of the fluid[?] of which the advective velocity is only a part.

The inability to model net mass diffusion and associated irreversible energy dissipation are not the only worrying consequences of combining advective and net diffusive fluxes into a single velocity $\boldsymbol{u}_m$. It has been argued that, by doing this, Fick's law for a constituent is applied relative to the net flux of all constituents when it is only applicable relative to a frame of reference external to the fluid.[?] Also, velocity associated with mass diffusion has questionable physical significance because where the concentration of a given specie $\to 0$, its diffusion velocity $\to \infty$.[?]

Instead, let us split the total mass flux density $\rho\boldsymbol{u}_m = \rho\boldsymbol{u} + \boldsymbol{j}_d$ where $\boldsymbol{u}$ is termed the advective velocity. If the diffusive flux is modelled by Fick's law, this leads to the following mass continuity equation:

$$\frac{\partial \rho}{\partial t} + \boldsymbol{\nabla} \cdot (\rho\boldsymbol{u}) - \boldsymbol{\nabla} \cdot (D_m\boldsymbol{\nabla}\rho) = 0. \tag{3}$$

This is the form of mass conservation equation proposed by Öttinger expressed in terms of u, not u_m. It is interesting to observe that the ratio R_{dc} of diffusive mass flux to advective mass flux can be expressed as

$$R_{dc} = \left| \frac{D_m \boldsymbol{\nabla}\rho}{\rho u} \right| = \frac{1}{A_\lambda \sqrt{\gamma} Sc} \frac{Kn}{Ma}, \tag{4}$$

where: the Mach number of the flow $Ma = |u|/c$ with c the speed of sound; the Schmidt number $Sc = \nu/D_m$; γ is the ratio of specific heats at constant pressure and volume; Kn is based on a Maxwellian mean free path $\lambda_M = A_\lambda \sqrt{\gamma}\nu/c$, with $A_\lambda = 16/(5\sqrt{2\pi}) \approx 1.28$. For argon gas, $\gamma = 5/3$ and the coefficient of self-diffusion of mass $D_m \approx 1.32\nu$,[?,?,?] so $Sc = 0.76$ and then $R_{dc} \approx 0.8 Kn/Ma$. In a planar shock in argon at Mach 4 upstream, $Kn \approx 0.275$ (see figure 3) and $Ma \approx 1.0$ local to the midpoint across the density profile, so $R_{dc} \approx 22\%$. The omission of mass diffusion from the governing equations will clearly lead to error at such a high R_{dc}. It could also be expected that R_{dc} is high in regions of low speed and moderate density gradient such as boundary layers and wakes, both regions where the departure from non-equilibrium behaviour is most pronounced in hypersonic flows.[?]

3. Momentum and energy conservation

Brenner's original hypothesis was that Newton's viscosity law should be expressed in terms of u , not u_m. Along with his own supporting analytical and experimental evidence, there is also the argument that velocity in Newton's viscosity law represents deformation of fluid volume and therefore cannot be based on a *mass average* velocity u_m.[?] The argument that velocity relating to mass diffusion has no physical significance[?] effectively precludes the use of u_m in Newton's viscosity law.

Öttinger additionally defines momentum density as ρu, not ρu_m, so that momentum relates purely to advective mass flux, not diffusive mass flux. This seems reasonable given that the advective flux is caused by mean translatory motion of molecules, associated with mechanical energy whereas the diffusive mass flux is caused by random motion of molecules associated with thermal energy. At the very least, if some momentum is attributed to mass diffusion, it must relate to a separate driving force independent of viscous forces associated with advective momentum.[?] The resulting equation can be alternatively viewed as the governing equation for momentum in the absence of a (net) diffusive mass flux. Following these arguments, the momentum equation is as in the standard governing equations (ignoring body forces) but expressed in terms of u, not u_m:

$$\rho \frac{Du}{Dt} = \frac{\partial(\rho u)}{\partial t} + \boldsymbol{\nabla} \cdot (\rho u_m u) = \boldsymbol{\nabla} \cdot P, \tag{5}$$

where the stress tensor $P = T - pI$ (defined as positive in tension), p is pressure and I the unit tensor. Newton's law is expressed as $T = 2\mu \, \text{dev}(D) + \kappa \, \text{tr}(D)I$ where κ is the bulk viscosity, the deformation gradient tensor $D \equiv \text{symm}(\boldsymbol{\nabla}u) \equiv (1/2)\left[\boldsymbol{\nabla}u + (\boldsymbol{\nabla}u)^{\text{T}}\right]$ and its deviatoric component $\text{dev}(D) \equiv D - (1/3)\,\text{tr}(D)I$. Note that the material derivative D/Dt is decomposed into the local rate of change $\partial/\partial t$ and the convective rate of change based on the local velocity of a fluid element that both advects and diffuses, i.e. u_m.

The derivation of a conservation equation for energy within a continuum framework that includes mass diffusion is more challenging. The energy equation derived using GENERIC,[?] for example, contains an unconstrained phenomenological parameter that has to be determined by theory or simulation and confirmed by experiment. Derivation through physical argument alone requires careful accounting of contributions of mass diffusion to mechanical and thermal energies and associated work. As a first approximation, we equate the rate of change of total energy to mechanical and thermodynamic energy fluxes (ignoring internal sources):

$$\rho \frac{DE}{Dt} = \frac{\partial(\rho E)}{\partial t} + \boldsymbol{\nabla} \cdot (\rho u_m E) = \boldsymbol{\nabla} \cdot (P \cdot u) - \boldsymbol{\nabla} \cdot j_e, \tag{6}$$

where the mechanical energy flux density ($P{\cdot}u$) relates to the advective velocity u only and heat energy flux is attributed to conduction only by Fourier's law $j_e = -k\boldsymbol{\nabla}T$ where k is the thermal conductivity. The total energy per unit mass E represents all mechanical and thermal energy contributions. Initial simulations of the shock structure problem showed the temperature-density separation, discussed in section 6.3, was strongly underpredicted when the E included a kinetic energy due to advective mass flux only. Instead, much better predictions were obtained when the kinetic energy was due to the total mass flux such that $E = e + |u_m|^2/2$, suggesting that net mass diffusion contributes to an additional source of energy beyond the internal energy.

4. Stability analysis

The same stability analysis was undertaken on the set of governing equations proposed in this work that previously highlighted limitations of Brenner's original modifications.[?] Following the procedures described previously,[?,?,?] it is
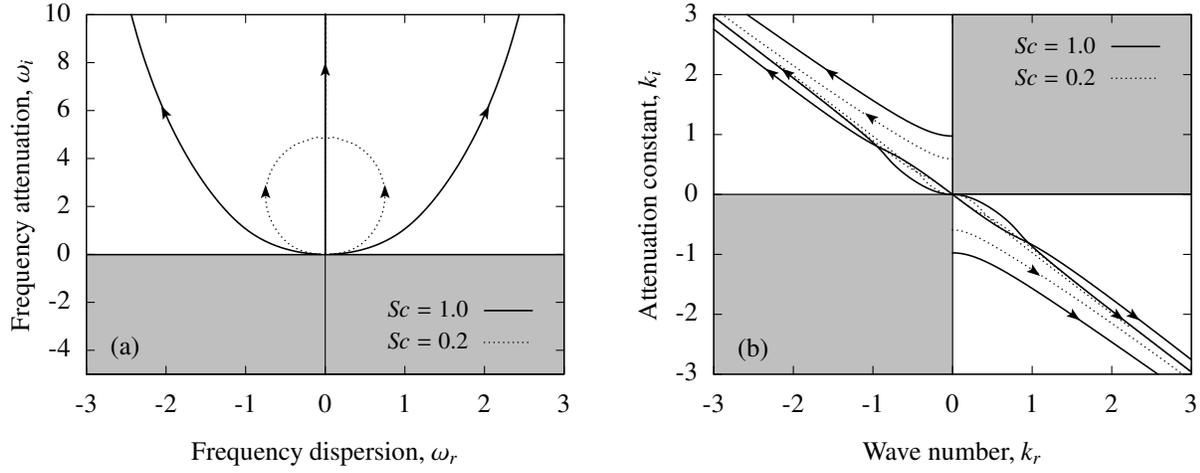
Figure 1: (a) temporal stability analysis; and, (b) spatial stability analysis of modified Navier-Stokes equations (grey shaded area indicates region of instability).

first assumed that the gas is monatomic and calorically perfect with $\gamma = 5/3$, Prandtl number $Pr = [\gamma R/(\gamma - 1)](\mu/k) = 2/3$, where R is the gas constant, and $\kappa = 0$. The governing equations from sections 2 and 3 are linearised in 1-dimension to produce the following non-dimensionalised perturbation equations:

$$\frac{\partial \phi}{\partial t'} + \begin{bmatrix} 0 & 1 & 0 \\ 1 & 0 & 1 \\ 0 & \frac{2}{3} & 0 \end{bmatrix} \frac{\partial \phi}{\partial x'} + \frac{\partial}{\partial x'} \left\{ \begin{array}{c} c' \\ \sigma' \\ q' \end{array} \right\} = 0, \tag{7}$$

where

$$c' = -\frac{1}{Sc}\frac{\partial \rho'}{\partial x'}, \quad \sigma' = -\frac{4}{3}\frac{\partial u'}{\partial x'} \quad \text{and} \quad q' = -\frac{5}{2}\frac{\partial T'}{\partial x'}. \tag{8}$$

We assume a solution to (7) of the form

$$\phi = \tilde{\phi} \exp\{i(\omega t' - kx')\}, \tag{9}$$

where $\tilde{\phi}$ is the amplitude of the wave, ω is its frequency and k its propagation constant. Equations (7) to (9) can be combined to produce a set of linear algebraic equations of the form

$$\mathcal{A}(\omega, k)\tilde{\phi} = 0, \tag{10}$$

for which non-trivial solutions require

$$\det[\mathcal{A}(\omega, k)] = 0. \tag{11}$$

For our modified governing equations, (11) yields the following characteristic equation:

$$6i\omega^3 + (23 + 6Sc^{-1})k^2\omega^2 - [10k^2 + (20 + 23Sc^{-1})k^4]i\omega - [(15 + 4Sc^{-1})k^4 + 20Sc^{-1}k^6] = 0. \tag{12}$$

If a disturbance in space is considered as an initial-value problem, k is real and $\omega = \omega_r + i\omega_i$ is complex. The form of (9) indicates that stability then requires $\omega_i \geq 0$. If a disturbance in time is considered as a problem of signalling from the boundary, ω is real and $k = k_r + ik_i$ is complex. For a wave travelling in the positive x direction, $k_r > 0$, and stability then requires that $k_i < 0$. For a wave travelling in the negative x direction, the converse is true: $k_r < 0$ and stability requires $k_i > 0$.

We examine temporal stability by solving (12) numerically for ω for values of k in the range $0 \leq k < \infty$. Trajectories of ω are plotted in the complex plane in figure 1(a). Stability was tested across a broad range of $0.2 \leq Sc \leq 1.0$ and sets of trajectories are plotted at the two extremes. In both cases the trajectories all lie within the region $\omega_i \geq 0$, indicating stability for all k.

We then turn to examine spatial stability by solving (12) numerically for k for values of ω in the range $0 \leq \omega < \infty$. Trajectories of k are plotted in the complex plane in figure 1(b) for the same values of Sc as before. In both cases, the trajectories do not violate the stability condition. The results therefore show stable solutions for the modified Navier-Stokes equations presented in this paper.

4

5. The shock structure problem and solution procedure

The shock structure problem presented in this paper concerns the spatial variation in fluid flow properties across a stationary, planar, one-dimensional shock in argon. We define the flow as moving at an advective speed u in the positive x-direction, with the shock located at $x = 0$; the upstream conditions at $x = -\infty$ are super/hypersonic and denoted by a subscript '1', downstream conditions at $x = +\infty$ are denoted by a subscript '2'. Shocks were simulated for a range of upstream Mach number $1.2 \leq Ma_1 \leq 11.0$ with the problem initialisation and viscosity model detailed previously,[?] but outlined briefly below.

The simulations adopted the same thermodynamic models and coefficients for argon used in earlier sections. The diffusive transport models were those previously described with the ratios of coefficients specified for argon, notably $Pr = 2/3$ and $Sc = 0.76$. The viscosity-temperature relation for argon was modelled[?] by a power law of the form $\mu = AT^s$ using an exponent $s = 0.72$ from independent experimental data. Since the results for this problem are historically presented in normalised form, the test problem was specified conveniently in a nondimensionalised form. The viscosity coefficient was set to $A = 1$, and in all simulations $p_1 = T_1 = 1$ was specified at the upstream boundary. A gas constant $R = \gamma^{-1} = 3/5$ was chosen so that $c_1 = 1$ and, simply, $u_1 = Ma_1$ for the particular simulation. At the downstream boundary, the normal gradient was specified as zero for all dependent variables except u_2 whose value was specified using the Rankine-Hugoniot velocity relation to maintain the shock stationary and fixed within the domain.

Simulations were performed using our solver, described in detail elsewhere,[?] developed using the open source Field Operation and Manipulation (OpenFOAM) software.[?] A solution domain of $33\lambda_{M1}$ was used in all simulations, wide enough to contain the entire shock structure comfortably. Initial results were obtained using the conventional Navier-Stokes equations that converged on a mesh of 800 cells to within 1% of the solution extrapolated to an infinitely small mesh size. The results presented in this paper were produced with a mesh of 2000 cells, corresponding to a mesh size of $\sim 0.017\lambda_{M1}$. Numerical solutions were executed until they converged to steady-state, at which point the residuals of all equations had fallen 5 orders of magnitude from their initial level.

Physical properties such as ρ and T vary continuously through the shocks from their upstream to their downstream levels over a characteristic distance of a few mean free paths. Results presented in this paper are normalised between 0 and 1 and denoted in the following by the superscript '$\star$', against distance through the shock, nondimensionalised by λ_{M1}. Where possible results are compared with actual experiments[?,?,?] rather than numerical Direct Simulation Monte Carlo (DSMC) data, since the latter requires certain assumptions relating to the form of the intermolecular force law.

6. Results

Figure 2(a) shows the variation of $\rho^\star$ and $T^\star$ through a shock of Mach 2.84 calculated using the Navier-Stokes and modified Navier-Stokes equations. The experimental density profile of Torecki and Walenta[?] is also shown. It is clear that the shock layer predicted by the conventional Navier-Stokes equations is too thin, whereas the modified Navier-Stokes equations produce good agreement with the experimental data. The main region of disparity is upstream of the shock layer (left hand side in the figure) where the prediction trails out and is flatter than the experimental data.
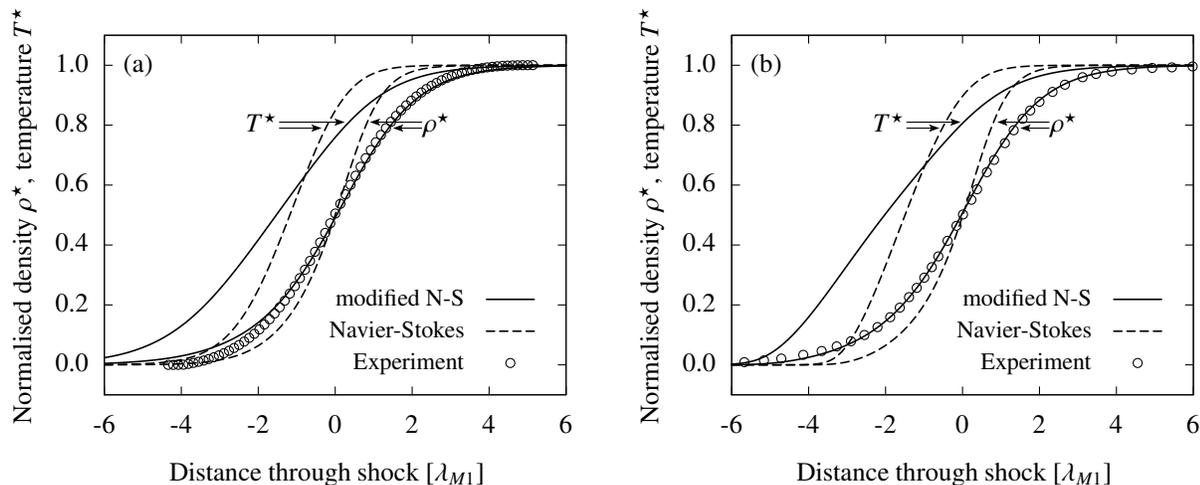

Figure 2: Simulated and experimental profiles of a stationary shock at: (a) Mach 2.84; (b) Mach 9.0
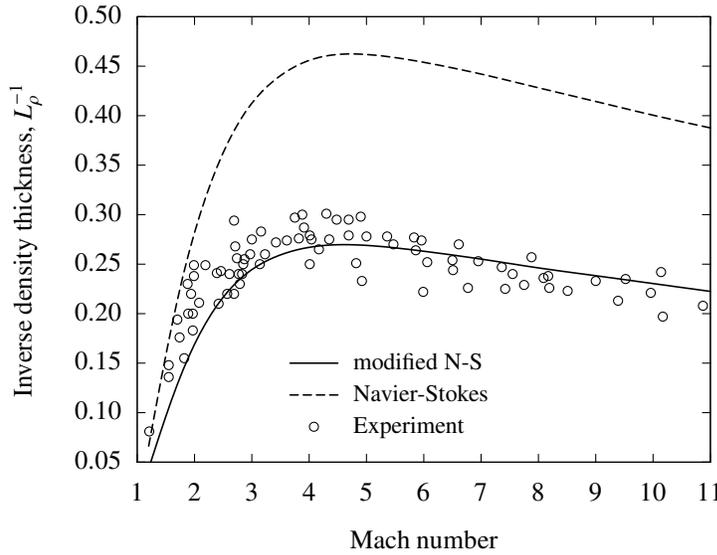
Figure 3: Simulated and experimental inverse density thickness (L_ρ^{-1}) data, versus shock Mach number.

Similarly, figure 2(b) shows the predicted profiles for a Mach 9.0 shock compared with experimental density data of Alsmeyer.[?] Again, standard Navier-Stokes equations produce a shock profile which is too thin when compared with experiment. However, the modified Navier-Stokes equations produce excellent agreement with the experimental data.

6.1 Inverse density thickness

Apart from direct comparison of calculated and experimental shock profiles, there are other shock parameters for which experimental and/or independent numerical data is available. The principal parameter is the non-dimensional shock inverse density thickness, defined as:

$$L_\rho^{-1} = \frac{\lambda_{M1}}{\rho_2 - \rho_1} |\boldsymbol{\nabla}\rho|_{\max} . \tag{13}$$

Comparing (1) and (13) it can be seen that, in the absence of a characteristic length scale L in an unconfined flow, the definition of Kn requires a characteristic dimension of a flow structure, in this case the actual thickness of the shock layer itself. Therefore L_ρ^{-1} has the interesting feature that it represents Kn for the shock structure case. Alsmeyer[?] reported the most comprehensive collection of experimental shock data, consisting of his own results and work published previously. Figure 3 shows L_ρ^{-1} for argon shocks up to Mach 11, comparing simulation results and experimental data from Alsmeyer[?] and other sources.[?,?] The Navier-Stokes equations predict shocks of approximately half the measured thicknesses over the entire Mach number range. As L_ρ^{-1} indicates Kn, this poor agreement is expected because, over most of this Mach number range, $Kn \sim 0.2$–0.3, beyond the accepted Kn limit of application of the Navier-Stokes equations. However, results from the modified Navier-Stokes equations match well with experiment, suggesting that correct prediction of density gradient has been attained by correct modelling of mass diffusion.

6.2 Density asymmetry quotient

Agreement of predicted and experimental shock inverse density thicknesses is not the only measure of the success of a model. As L_ρ^{-1} depends on the density gradient at the profile midpoint alone, it does not express anything about the overall shape of the profile. Instead, a second parameter that can be used to describe the shock profile, and for which experimental data is available, is the density asymmetry quotient Q_ρ. This is a measure of how skewed the shock density profile is relative to its midpoint. It is defined for a 1-dimensional profile of normalised density, $\rho^\star$, centred at $\rho^\star = 0.5$ on $x = 0$, as

$$Q_\rho = \frac{\int_{-\infty}^{0} \rho^\star(x)\, dx}{\int_{0}^{\infty} [1 - \rho^\star(x)]\, dx}. \tag{14}$$

A symmetric shock would consequently have $Q_\rho = 1$, but real shock waves are not completely symmetrical about their midpoint. First, their general form is skewed a little towards the downstream. Then, the flattened, diffusive region, that

6

Figure 4: Asymmetry quotient (Q_ρ) versus shock Mach number.

Figure 5: Simulated and DSMC profiles of a stationary shock at Mach 11

extends upstream of the shock profile, tends to increase Q_ρ with increasing Mach number. Figure 4 shows experimental data[?] in which Q_ρ increases fairly linearly from ~ 0.9 at around Mach 1.5, through unity at around Mach 2.3, to ~ 1.15 at Mach 9.

Results from the Navier-Stokes equations do not agree well with experimental data: $Q_\rho > 1.0$ at Mach 1.2, and rapidly increases with Mach number with the profile sharpening downstream of the shock until by Mach 4 it levels off to $Q_\rho \approx 1.4$, compared to ~ 1.03 from experiment. The modified Navier-Stokes equations similarly overpredict Q_ρ at Mach 1.2 but, with increasing Mach number, Q_ρ quickly levels off at ~ 1.1 so that, by Mach 6, Q_ρ matches well with experiment and the density profiles are very well predicted, e.g. for the profile at Mach 9 in figure 2(b).

6.3 Temperature-density separation

In a shock, the density rises from its upstream value to its downstream value behind the temperature, due to the finite relaxation times for momentum and energy transport. Experimental data for this phenomenon is scarce due to the difficulty in measuring temperature profiles, but results from DSMC simulations provide such data. Figure 5 shows a comparison of profiles for a Mach 11 shock from our simulations and those calculated using DSMC.[?] DSMC clearly predicts a much larger separation distance between density and temperature profiles than conventional Navier-Stokes equations. The modifications to Navier-Stokes do increase the temperature-density separation, though not to the extent of the DSMC predictions. The temperature profile predicted by the modified Navier-Stokes equations is generally less diffusive than that predicted by DSMC, particularly at the upstream end.

7. Conclusions

It is accepted that the conventional Navier-Stokes equations fail to predict correct shock structures above about Mach 2, where the flow falls within the intermediate-*Kn* regime. Brenner's modifications to Navier-Stokes improve the predictions of shock structures considerably[?] but only with the somewhat arbitrary choice of diffusion coefficient $D_v = v$ based on an upper limit above which the equations produce unphysical solutions and, at even higher D_v, become unstable.

Rather than basing the modifications to Navier-Stokes on the notion of a diffusive volume flux, we instead present modifications due to the inclusion of a diffusive mass flux. The resulting set of governing equations deliver a similar improvement over conventional Navier-Stokes in reproducing the trends in the experimental and DSMC data, and in the case of the inverse density thickness produce a very good match. The new model uses a *known* coefficient for self-diffusion of mass for argon and the equation set does not exhibit the unphysical and unstable behaviour previously observed with Brenner's modifications. The new equation set is extremely easy to solve: it contains none of the higher order derivatives of the Burnett family of models, nor the second derivative of density contained within Brenner's original model; indeed, the addition of a diffusive term to the mass conservation equation makes the new set arguably easier to solve numerically than the conventional Navier-Stokes equations themselves.

While it is important not to draw strong conclusions based on just one test case, the results are generally encouraging. Our future aims are: to test this model further on a number of benchmark cases ranging from high-speed flows encountered in hypersonics to specific studies of diffusion phenomena such as thermophoresis, and to refine and develop the models accordingly.

Acknowledgements